

## Time-frequency Analysis of Migrating Zooplankton in the Terra Nova Bay Polynya (Ross Sea, Antarctica)

Paola Picco<sup>1</sup>, M. Elisabetta Schiano<sup>2</sup>, Sara Pensieri<sup>3</sup>, Roberto Bozzano<sup>3</sup>

<sup>1</sup> Istituto Idrografico della Marina, Passo dell'Osservatorio 4, 16134 Genova, Italy

paola.picco@persociv.difesa.it

<sup>2</sup> National Research Council of Italy - Institute of Marine Science, Via de Marini 6, 16149 Genoa, Italy

<sup>3</sup> National Research Council of Italy - Institute of Intelligent Systems for Automation, Via de Marini 6, 16149 Genoa, Italy

### Abstract

An upward-looking 150 kHz narrow-band acoustic Doppler current profiler was operated in Terra Nova Bay (Ross Sea, Antarctica) from 5 February 2000 to 16 January 2001 to monitor marine currents. The instrument sampled the upper 160 m of the water column with a time resolution of 1 hour. Although the experimental setup was not specifically designed to assess zooplankton and fish distributions and behaviour, the Acoustic Doppler Current Profiler ancillary data provided useful information regarding the diel vertical migration of these acoustic targets. A time frequency analysis of the mean backscatter strength time series was conducted using a 240 h-wide window with a 1 day step. Assuming that the 24 hour period peak is associated with zooplankton diel vertical migration, the amplitude of the power spectral energy on this band was extracted from each spectrum and the time series of amplitudes was analysed. The migration signal was very weak during summer, December to January, but was evident at the beginning and end of the polar night. Interestingly, the results indicated four “migratory blooms,” the first at the end of August and the others approximately every three weeks subsequently, ending at the end of October. The daily migration was found to have a good relation with the solar cycle, while it was apparently uncorrelated with the moon phase. Migration patterns in the upper and the lower ocean layers displayed significant differences. Due to the lack of contemporary in-situ net samples, the results are more qualitative than quantitative; nonetheless, they demonstrate the validity of the method to extract relevant information even when applied to data obtained from a non-devoted low-resolution system. This may be of particular interest in polar areas where it is difficult to perform continuous biological monitoring but where a long time series of acoustic Doppler current profiler data is available.

**Keywords:** ADCP, polynya, spectral analysis, zooplankton migration, Antarctica, Ross Sea, Terra Nova Bay

## 1. Introduction

Terra Nova Bay is located on the western side of the Ross Sea, bounded on the south by the Drygalski Ice Tongue and characterized by the presence of a recurrent, latent heat polynya with a mean size of approximately 6000 km<sup>2</sup> (Kurtz and Bromwich, 1985; Van Woert, 1999) that persists during winter. This area is of particular interest for climatic studies because dense water formed during winter, the High Salinity Shelf Water (HSSW), contributes to the Antarctic Bottom Water (ABW) that is part of the global thermohaline circulation (Assmann and Timmermann, 2005; Jacobs, 2004; Jacobs et al., 1985). It is also host to an important nursery of the Antarctic silverfish (*Pleuragramma antarcticum*) (Vacchi et al., 2012), a colony of Adélie Penguins (*Pygoscelis adeliae*) in Adélie Cove, and the large Emperor Penguin (*Aptenodytes forsteri*) reserve at Cape Washington (Kooyman et al., 1990). Due to its high ecological value, Terra Nova Bay is an Antarctic Special Protected Area (Antarctic Treaty Secretariat, 2003). For all of these reasons, the area has been the object of scientific investigations since the beginning of the Italian Antarctic Program and was selected as the location for the Antarctic scientific base Mario Zucchelli Station.

Polynyas are special areas for polar marine life because they are almost entirely free from ice and, at the end of the polar night, solar radiation immediately penetrates the water, producing early warming and irradiance that can stimulate relatively early seasonal phytoplankton production (Tremblay and Smith, 2007). This high primary productivity sustains a food-rich area for higher trophic levels (Hopkins, 1987; Karnowsky et al., 2007), attracting animals as large as marine mammals, which also take advantage of these ice-free areas for breathing.

Zooplankton can be regarded as the trophic link between primary producers and higher trophic levels. Despite their importance, studies on this fundamental component of the Antarctic ecosystem are still limited, largely due to the lack of a long time series with continuous data. In fact, for most of the year, the sea-ice coverage does not allow for in-situ sampling. In the Ross Sea and in Terra Nova Bay, several experimental studies have been carried out during the short austral summers (Azzali and Kalinowski, 2000; Carli et al., 2000; Pane et al., 2004), and trophic models have been developed for these regions (Pinkerton et al., 2010; Tagliabue and Arrigo, 2003); however, few long-term observations are available for the whole year. Thus, much important information about the zooplankton abundance during the entire annual cycle is gathered through indirect observations, such as data obtained from the analysis of faecal pellets collected in sediment traps (Accornero et al., 2003).

Acoustic measurements are widely used to remotely observe oceans, and dedicated instrumentation on a wide range of frequencies is now available for the detection of zooplankton and fishes of different sizes (Brierley et al., 2006; Briseño-Avena et al., 2015; Lemon et al., 2012). An additional

source of acoustic data stems from the by-products of Acoustic Doppler Current Profilers (ADCPs). Despite being designed to perform for 3D current measurements, ADCPs also provide ancillary data, specifically the echo intensity profile, that is dependent on the presence of scatterers (e.g., biomass, sediment, bubbles) in the water column. This type of data has been successfully applied in different scientific investigations (Gostiaux and van Haren, 2010) for the detection of zooplankton migration (Flagg and Smith, 1989; van Haren, 2007), suspended sediments (Jourdin et al., 2014; Russo and Boss, 2012), and sea surface conditions (Hyatt et al., 2008; van Haren, 2001). The use of ADCP data could be a great advantage for long-term investigations in polar areas, where direct sampling and satellite measurements are hampered by the presence of sea-ice.

During 2000-2001, in the framework of the Italian Program of Antarctic Research (PNRA, 2001), ADCP measurements were made in Terra Nova Bay to investigate the dynamics in the upper layers of the ocean (Cappelletti et al., 2010). To investigate the zooplankton dynamics of the region, particularly with regard to their migration patterns, occurrence and seasonal cycle, the echo intensity data collected by ADCP were examined. The methods used here allow ADCP ancillary time series data to be analysed more objectively and quantitatively than other methods that are primarily based on visual and qualitative assessments.

The lack of concurrent biological samples did not allow for an in-situ calibration of the raw echo intensity data provided by the ADCP. Consequently, the application of spectral and time-frequency methods to the backscatter strength data is only suitable for identifying the vertical migratory patterns of zooplankton. Despite this, the results can still give provide indications of the behaviour of some specific taxa in the area during the experiment. Additionally, this analytical method can be applied to the historical time series of ADCP data collected in the area for other purposes, furthering the knowledge of Antarctic zooplankton behaviour, especially during winter periods when net samples cannot be taken.

## **2. Materials and methods**

### **2.1 Experimental setup**

An oceanographic mooring (D2) equipped with an upward-facing 150 kHz narrow-band ADCP was kept in operation in Terra Nova Bay (74°55.11' S; 164°20.4' E) from 5 February 2000 to 16 January 2001 (Figure 1). The mooring was deployed at a depth of 600 m, and an ADCP was mounted at a depth of 178 m and set to sample the water column up to the surface at a vertical resolution of 16 m. The middle of the deepest level was 160 m. The ping frequency was set at one

minute. To reduce the standard deviation of each measurement, the instrument was programmed to provide the average of the output data obtained over a one hour period.

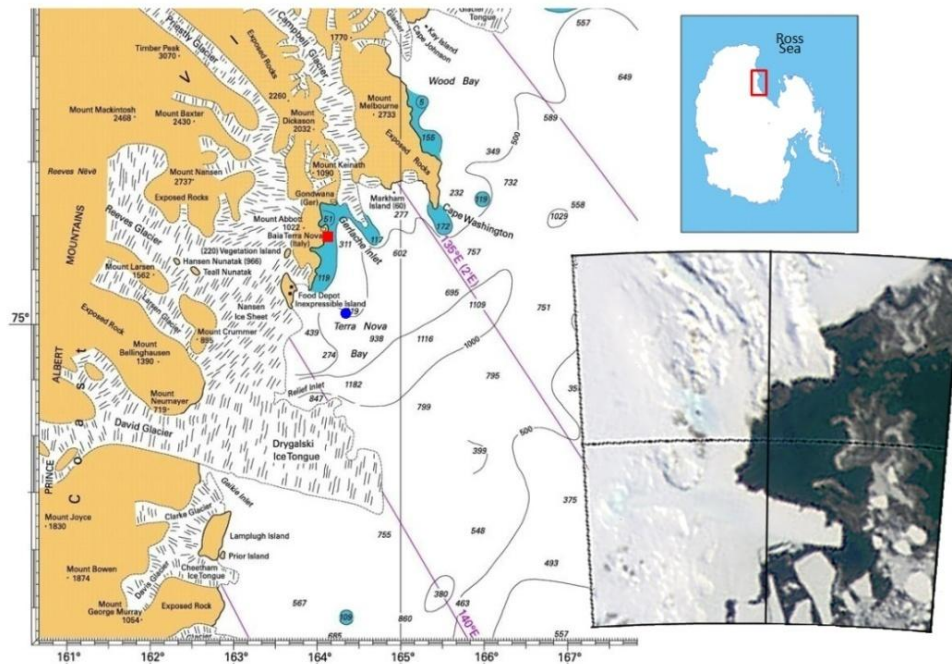


Figure 1. Map of the study area. The dot and square correspond to the position of the D2 mooring and the Antarctic Weather Station ENEIDE, respectively. The satellite image, taken on 26 December 2001, was provided by the Sea-viewing Wide Field-of-view Sensor (SeaWiFS) Project from NASA and shows the Drygalski Ice Tongue and polynya.

Two Aanderaa RCM7 Eulerian current meters were also mounted on the same mooring, at 89 m and 179 m. A second mooring (D1), equipped with Eulerian current meters and temperature and salinity sensors, was located in the same area ( $75^{\circ}07.61' \text{ S}$ ;  $164^{\circ}27.10' \text{ E}$ , depth of 1100 m) and provided a one year time series of temperature and salinity from fixed sensors at 126 m and 526 m. During the mooring deployment and recovery, CTD casts were performed to provide summer temperature and salinity profiles for the area. The environmental conditions during the study period were obtained from the available oceanographic, meteorological and satellite observations.

The meteorological parameters, including wind speed, wind direction, atmospheric pressure and air temperature, were collected by the Antarctic Weather Station ENEIDE ( $74^{\circ}42' \text{ S}$ ;  $164^{\circ}6' \text{ E}$ ), the closest land-based meteorological station to the study area. Direct solar radiation measurements were available only for early November to mid-February, so the theoretical no-sky solar radiation was computed using the MatLab<sup>®</sup> air-sea toolbox version 2.0:8/9/99. This parameter was used to infer the seasonal and daily cycle of irradiance and ranges between 0 and  $884 \text{ W/m}^2$  at the latitude of this mooring. Sea ice concentration data at a 25-km resolution between  $164^{\circ} \text{ E}$  to  $165.5^{\circ} \text{ E}$  and  $74.5^{\circ} \text{ S}$  to  $75.5^{\circ} \text{ S}$  were obtained from the Nimbus-7 Scanning Multichannel Microwave

Radiometer (SMMR) and the Defence Meteorological Satellite Program (DMPS, USA) SSM/I passive microwave analysis archived at the National Snow and Ice Data Centre (Cavalieri et al., 2008).

## 2.2 Environmental conditions during the study

Sea-ice coverage satellite data allowed for the generation of a rough estimate of the temporal evolution of the Terra Nova Bay polynya extension and, consequently, allowed for a determination of when the sea surface on the mooring location was ice-free. The temporal data of the sea-ice concentration were extracted from the pixel closest to the position of the mooring and indicated that the ice never completely covered the area during the study period. The most sea ice coverage occurred during June to October, but was less than 20% in February. The strong katabatic westerly winds associated with an increase in air temperature supported a large polynya area, while the sea ice concentration expanded after periods of low wind, such as the second half of May and mid-March.

The sea currents were mainly barotropic, moving northeast at a mean speed of approximately 30 cm/s, (Cappelletti et al., 2010). From February to April, they had a slower speed and moved eastward. In the upper 16 m, the horizontal currents were strongly wind-driven and reached hourly mean velocities of almost 70 cm/s. In the surface layer, the vertical velocities were very strong, with peaks up to 20 cm/s, and highly variability, particularly in December, when, notwithstanding the low wind intensity, the vertical motions were intensified by thermohaline forcing due to early ice melting. At deeper depths along the entire water column, the greatest vertical velocities occurred between June and October. These corresponded with increased salinity associated with episodes of dense water formation, while slower vertical velocities characterized the summer season from December to February.

The temperature and salinity time series available at 126 m showed evidence of mixing with fresh water derived from ice melt. The salinity reached a minimum (34.54 psu) at the end of May, while the maximum (34.76 psu) occurred on October. The sea water temperature was constant at -1.92 °C from late March to the end of November. As a result of the ice melt, summer CTD casts showed a surface layer with a salinity of less than 34 psu and slightly warmer waters (just above zero degrees) that enhanced the generally weak vertical stratification. During winter, uniform temperatures hovered around the freezing point, while strong mixing and dense water formation made the water column vertically unstable. It should be noted that at this latitude, the polar night lasted from April 29 to August 11 and the midnight sun period was from November 3 to February 8.

## 2.3 ADCP data quality control

A detailed analysis of the data quality control for the ADCP data can be found in Cappelletti et al. (2010).. In particular, the pitch, roll and tilt angle data were all below the limits specified by the manufacturer, which ensured that the mooring maintained its vertical position despite the strong currents in the region. In addition, the percent of good data confirmed the high quality of the collected measurements. A further quality check to detect outliers, gross errors, and incoherent data was performed using the echo intensity data before computing the backscatter strength ( $S_v$ ). Specifically, it verified that each measurement fulfilled the following conditions to obtain a good signal to noise ratio:

$$K_c*(E-E_{noise})>10$$

where  $E_{noise}$  is the minimum recorded raw value in the experiment (here 55 counts),  $E$  is the raw echo intensity and  $K_c$  is the conversion factor from the echo intensity expressed in counts to dB. All of the observations that did not satisfy the above conditions were discarded. Additional tests showed that the Eulerian current meter located on the same mooring at 86 m did not affect the ADCP measurements.

The mean profile of echo intensity data for each beam signal usually decreases as the distance from the source increases. The air-sea interface also strongly affects the bins closest to the sea surface. Therefore, as suggested by the manufacturer, data from the bins located at the air-sea interface were discarded.

## 2.4 Backscatter strength computation

Hourly data of the mean backscatter strength were computed according to the formula from the sonar equation (RD Instruments, 1998) according to the protocol in Blanc et al. (2008). The echo intensity amplitude depends on the instrument's technical characteristics and on the sampling site. The formula returns the absolute physical data (backscatter strength), allowing for a comparison of different data sets (Fielding et al., 2004).

Because there were no concurrent profiles of temperature and salinity during the study period, constant values of the sound speed velocity and sound absorption coefficients were obtained from the data collected by the mooring and from the summer CTD casts. Constant values were adopted after determining that there was a low impact of temperature and salinity variability on the computation of these parameters.

During the study period, the temperature variation in the upper layers was limited to a few degrees,

while the salinity changed less than 1 psu. These variations only affected the computation of the sound speed in the upper 50 m during the short melting period. Moreover, the effects of increased depth on the sound speed were limited to 2 m/s as the water column sampled by the ADCP was between the surface and 160 m.

The absorption coefficient of water was computed according to Ainslie and McColm (1998) using constant values of  $T=-1.9$  °C,  $S=34.6$  psu,  $pH=8$ ,  $z=80$  m. The limited variability of these parameters only has a small influence on the value of the coefficient. In fact, a difference of 1 °C in temperature results in a coefficient variation of less than 3%, while the effects of salinity and depth variations are also negligible.

An additional test was performed to compare the Sv profile from the beginning of the experiment (February 5, 2000), using a temperature and salinity profile collected close to the mooring just before deployment. Although the CTD profile was performed at the end of the melting season when maximum vertical variability is expected, the difference between the CTD-derived and constant-value profiles was negligible, less than  $10^{-3}$  of the signal strength.

The computation of Sv was performed for each beam and then for the four sets, as follows

$$S_v = 10 \log \left( \frac{4.47 \cdot 10^{-20} K_2 K_s (273 + T_x) (10^{(K_c(E-E_R)/10)} - 1)}{C' P K_1 10^{-2\alpha R/10}} R^2 \right)$$

$$R = \frac{B + \left( \frac{P-D}{2} \right) + nD + \frac{D}{4} \frac{C'}{C}}{\cos \vartheta}$$

where

Sv is the backscatter strength in dB re  $(4\pi m)^{-1}$ ,

R is the range of the scatterers along the beam (slant range),

$\alpha=0.0298$ , which is the absorption coefficient of water (dB/m),

$\vartheta = 20^\circ$ , which is the beam angle of the ADCP,

$n = 1...10$ , which is the cell number,

$B = 2$  m, which is the blank distance,

$D = 16$  m, which is the depth of the cell,

$C = 1442$  m/s, which is the sound speed at the ADCP,

$C' = 1440$  m/s, which is the average sound speed of the water column,

E is the raw echo intensity measured by the ADCP,

$E_R = 55$  counts, which is the reference level for the echo intensity obtained as the minimum recorded value of the bin closest to the surface,

$K_c = \frac{127.3}{T_x + 273}$  dB/count is the conversion factor for echo intensity,

$K_2 = 3.6$ , which is the system noise constant as provided by the manufacturer,

$K_s = 4.17 \cdot 10^5$ , which is a constant depending on the ADCP frequency,  
 $K_1 = 3.9 \text{ W}$ , which is the transmit power as provided by the manufacturer,  
 $P = 16 \text{ m}$ , which is the transmit pulse length,  
 $T_x = -1.9 \text{ }^\circ\text{C}$ , which is the sea temperature at the transducer.

## 2.5 Time frequency analysis

Time frequency analysis is a powerful tool that can be used to investigate the occurrence and temporal evolution of phenomena that can be identified by a specific periodic behaviour. The method proved to be useful for analysing meteorological and oceanographic data (Soares and Cherneva, 2005). It was successfully applied to a long-term ADCP backscatter dataset to study zooplankton migration characterized by strong daily and/or sub-daily variability (Bozzano et al., 2014).

Time frequency analysis of the present backscatter data was performed for a selected total of 240 sample hours with a centred window moving at a 24 h time step. A ten-day interval was the best compromise to resolve the frequencies of interest. A wider window would have ensured a better spectral resolution, but would have also reduced the temporal resolution, as each spectrum would have been representative of a longer interval. Before the FFT analysis, each sample was de-trended to limit the contribution of the lowest frequencies. Data were processed at all bin levels.

The backscatter signal from zooplankton and ichthyoplankton migration was assumed to be a 24 h period square wave-like form. The contribution of the twilight migration, typical of some zooplankton that repeat their migration from the surface to a depth twice per day, is generally less important and can be identified by a 12 h minor peak in the spectrum. However, as is the case for the polar regions, the length of the night and day dramatically changes throughout the year, which may influence the daily migration cycle, leading to a highly asymmetric 24 h wave. As a consequence, secondary peaks on both even and odd harmonics characterize the resulting spectrum, which could mask the contribution of the twilight zooplankton migration. We illustrate the challenges in interpreting the data with the following three idealized situations. First, the signal is a symmetric 24 h period square wave (duty cycle 50%). Second, the signal is an asymmetric 24 h period square wave (duty cycle 62%). Third, the signal is the sum of two symmetric square waves (duty cycle 50%), one with a 24 h period and the other with a 12 h period, leading to a 30% reduction of the amplitude and a 6 h phase shift. Random noise with an amplitude of one-tenth of the 24 h square wave amplitude was added in all three cases (Figure 2, left column). Then, FFT analysis was performed on the three samples (Figure 2, right column). A 12 h peak appeared in the FFT spectrum of the second case. This was due to the effect of the 62% duty cycle of the original



24 h square wave and was larger than the peak of the third case, which results from the real presence of a 12 h component in the signal.

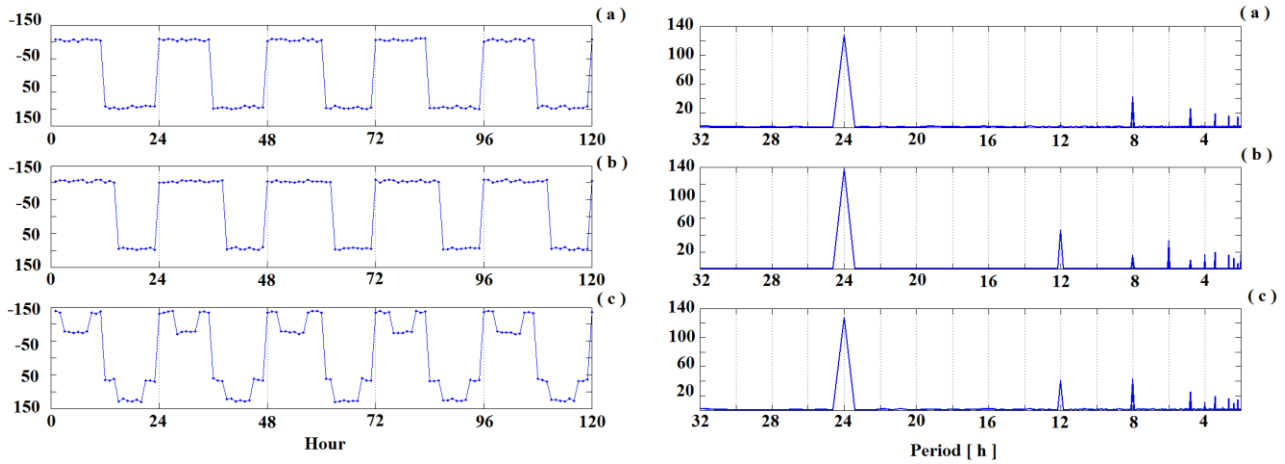


Figure 2. (Left column) Simulated signal and (right column) relative FFT spectrum for the three cases: a) 24 h period square wave with a duty cycle=0.5; b) 24 h period square wave with a duty cycle=0.62; c) sum of 24 h and 12 h period square waves with a duty cycle=0.5.

Therefore, the interpretation of the results may be ambiguous and require particular attention. To avoid an incorrect interpretation of the data, it is necessary to carefully analyze the spectrogram of the 12 h signal and to compare the 12 h spectrogram to that obtained at 24 h to identify the periods when the signal is significant; if necessary, visual inspection of each selected period can be used to help identify these signals.

### 3. Results

#### 3.1 Seasonal variability

The echo intensity data measured by acoustic devices were the result of the amount and type of scatterers present in the volume of water, particularly suspended sediments, biomass, and bubbles. It is known that strong winds, ocean fronts and turbulence, as well as the presence of the sea surface or bottom interfaces, can all affect the backscatter signal in different ways (Visbeck and Fisher, 1995). Therefore, the time series of the daily average backscatter strength profiles (Figure 3) was first analysed to identify the possible causes influencing backscatter intensity.

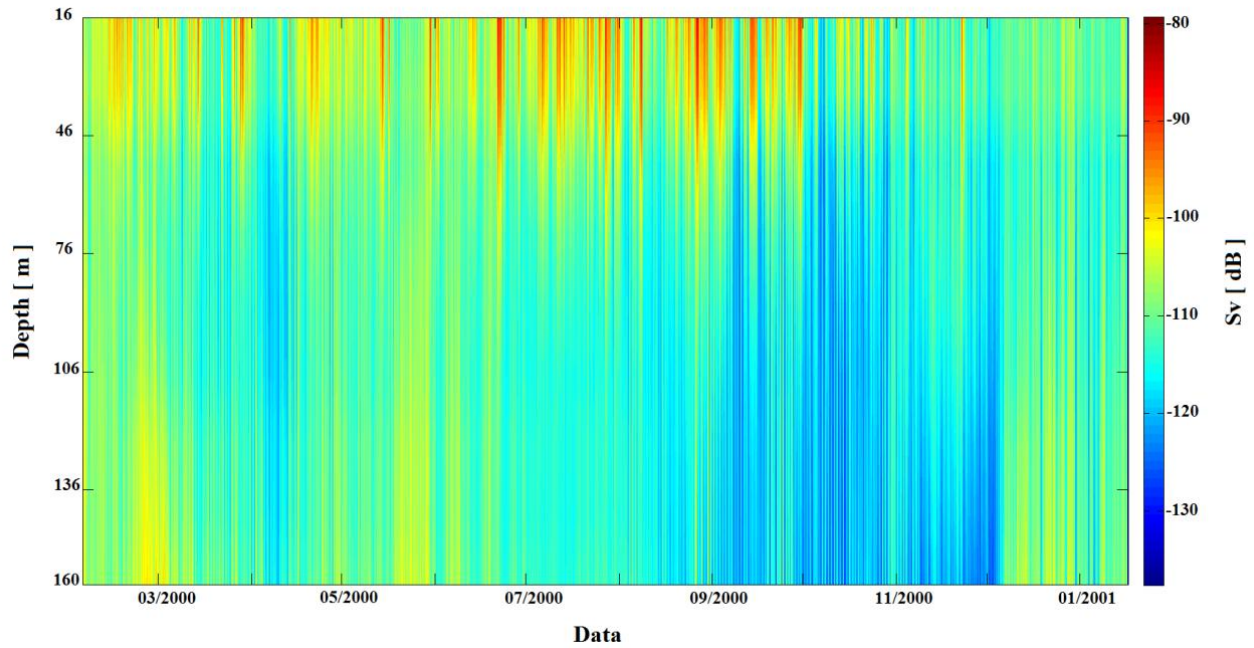


Figure 3. Temporal variability of the acoustic backscatter strength during the entire study period.

The results of the correlation analysis between the data collected in the ten layers (Table 1) showed that the mean patterns of acoustic backscatter in the upper 72 meters of the water column differed from those in the layers between 104 and 168 m.

Higher variability and values of acoustic backscatter occurred in the surface layers (16 m to 50 m), particularly during winter. There was a good correlation between wind kinetic energy peaks and backscatter strength at a depth of 16 m, especially from February to June, when the correlation of the two series is greater than 0.5 (Figure 4). However, the strongest winds, such as those during winter months, do not seem to affect the echo intensity, as was expected. This may be due to the effects of sea ice at the surface modifying the relationship between wind and the acoustic backscatter strength.

Depth limits of each bin [m]	152-168	136-152	120-136	104-120	88-104	72-88	56-72	40-56	24-40	8-24
Bin Bin	1	2	3	4	5	6	7	8	9	10
1	1 0	0.94 0	0.87 0	0.73 0	0.6 0	0.49 0	0.26 0	0.52 0.0007	-0.04 0.0043	-0.12 0.9972
2		1 0	0.97 0	0.86 0	0.72 0	0.57 0	0.28 0	0.03 0.0057	-0.09 0.3779	-0.13 0.5776
3			1 0	0.95 0	0.85 0	0.70 0	0.38 0	0.08 0.0009	-0.08 0.4613	-0.10 0.6426
4				1 0	0.96 0	0.82 0	0.51 0	0.14 0	-0.05 0.2943	-0.07 0.8878
5					1 0	0.93 0	0.64 0	0.27 0	0.03 0	0.02 0
6						1 0	0.86 0	0.53 0	0.28 0	0.26 0
7							1 0	0.86 0	0.67 0	0.61 0
8								1 0	0.93 0	0.86 0
9									1 0	0.92 0
10										1 0

Table 1. Correlation matrix of backscatter strength. Correlation coefficients, R and P values computed with an alpha set to 0.05, are shown in the first and second rows of each cell, respectively. Values lower than  $10^{-4}$  are rounded to 0.

In fact, the decrease in the backscatter strength during low wind periods, particularly beginning in December, which had the lowest wind intensities, is evident (Figure 4). Seasonal trends were opposite at deeper depths, with the greatest values recorded during summer, particularly in December and January, and, to a lesser degree, through mid-March (Figure 3). High values also occurred during the last two weeks of May, following a period characterized by low backscatter intensity. Low values were more frequent in April and between September and late November. Relative minima were common in all layers throughout the study period.

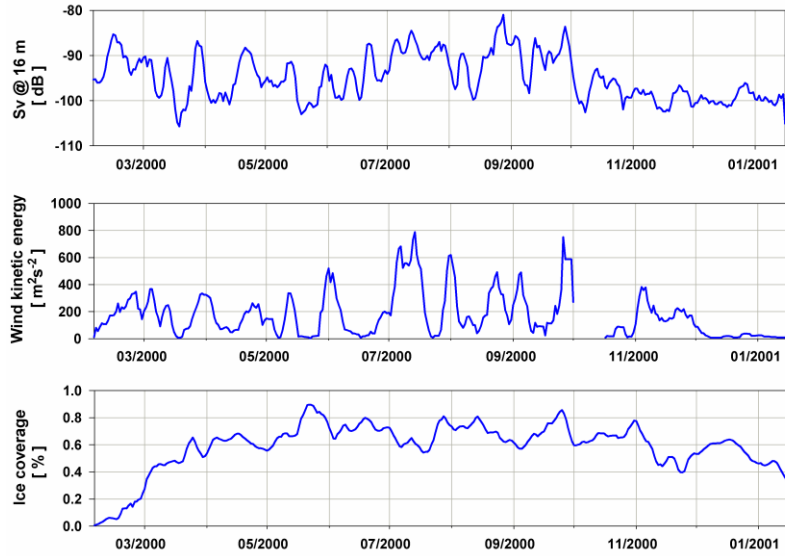


Figure 4. Time series of the daily backscatter strength at 16 m as well as wind kinetic energy and sea ice coverage during the study period.

To analyse sub-daily variability, a spectral analysis of the entire series of the hourly mean backscatter of each level for 34 adjacent subsamples for 240 h each was performed and then averaged to increase the confidence level (Figure 5). Aside from the 16 m level, which was dominated by a red spectrum with less-pronounced peaks, the averaged spectra had almost the same features, with a maximum at the 24 h harmonic, a secondary peak at 12 h and a series of peaks at higher harmonics.

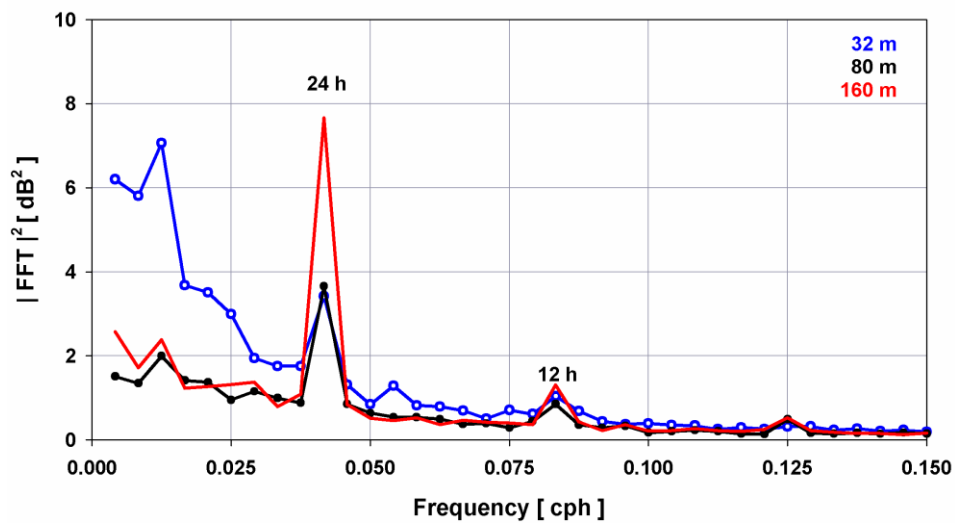


Figure 5. Power spectrum of the backscatter strength at 32 m (solid line, empty dots), 80 m (solid line, filled dots) and 160 m (solid line) as the average of the FFT performed on 34 adjacent subsamples for 240 h (ten days).

To evaluate the temporal evolution of the two main harmonics, a time frequency analysis was performed, as described in Section 2.5. For each depth, the amplitudes of the 24 h and the 12 h harmonics were extracted to obtain a temporal series of the two amplitudes. The vertically integrated time series of the amplitudes, superimposed on the computed solar cycle and moon phase, are shown in Figure 6. Both time series illustrate the main features of the migratory phases of zooplankton in the area and correlate well with the annual solar cycle, although there was no clear correspondence with the full moon.

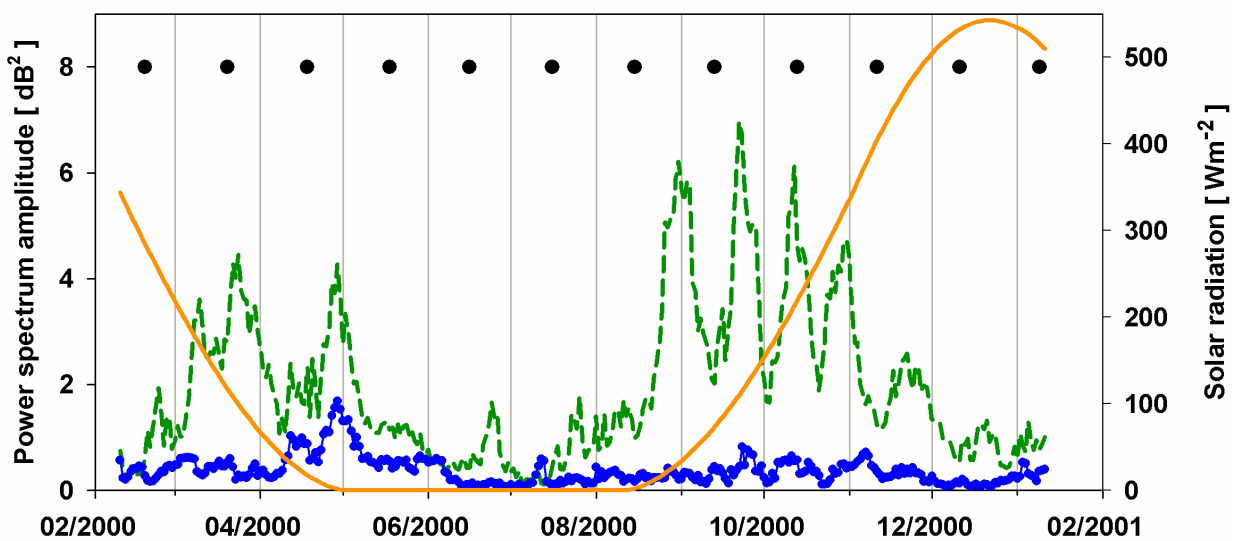


Figure 6. Temporal evolution of no-sky solar radiation (solid line) and the vertically integrated (from 8 to 176 m) backscatter amplitude of the 24 h (green dashed line) and the 12 h (blue dotted line) harmonics. Black dots represent a full moon at the mooring site.

Four major episodes characterized the zooplankton seasonal migratory patterns. The first occurred at the end of August and lasted for approximately ten days, while the other episodes occurred approximately every three weeks, ending in October. Vertical daily migration was strongly reduced from late November to early March, when the solar radiation reached its greatest values and the day length was at its maximum. From early May to mid-August, during the polar night (at the mooring latitude the polar night lasts from May 1<sup>st</sup> to August 13<sup>th</sup>), vertical migration was also reduced with the exception of a small peak near the end of June. The amplitude of the 12 h signal was quite low even though it corresponded with some of the highest 24 h peaks. The main peak occurred at the end of April, which corresponded with a relative maximum in the 24 h amplitude time series. Analysis of the spectrograms highlights some relevant differences between the upper (16-100 m)

and lower (100-168 m) levels. Three representative depths are presented in Figure 7. The time series of 24 h amplitudes was correlated within the 96 m to 160 m depth interval (correlation coefficients 0.6-0.92). However, they were completely uncorrelated between the surface and 64 m (coefficients  $< 0.2$ ). The time series showed a strong correlation at 64 m, with the adjacent depths, 80 m and 48 m, reaching a correlation coefficient value of 0.7.

While the major four 24 h peaks dominated in the deeper layers (100-168 m), the signal at 80 m (Figure 7) experienced the first maximum during the second half of September, corresponding with the second major peak at the deeper levels, followed by minor peaks approximately every two weeks. At the same depth, maxima of comparable amplitudes lasting for approximately two weeks occurred between March and June, with the most significant maxima at the beginning of May. The amplitude of the 12 h harmonic was generally lower, with a different temporal evolution. Twilight migration appeared to dominate in April and May and at intermediate depths, between 64 and 112 m. Some 12 h peaks of particular importance occurred in May at 80 m and in mid-November at the deepest levels.

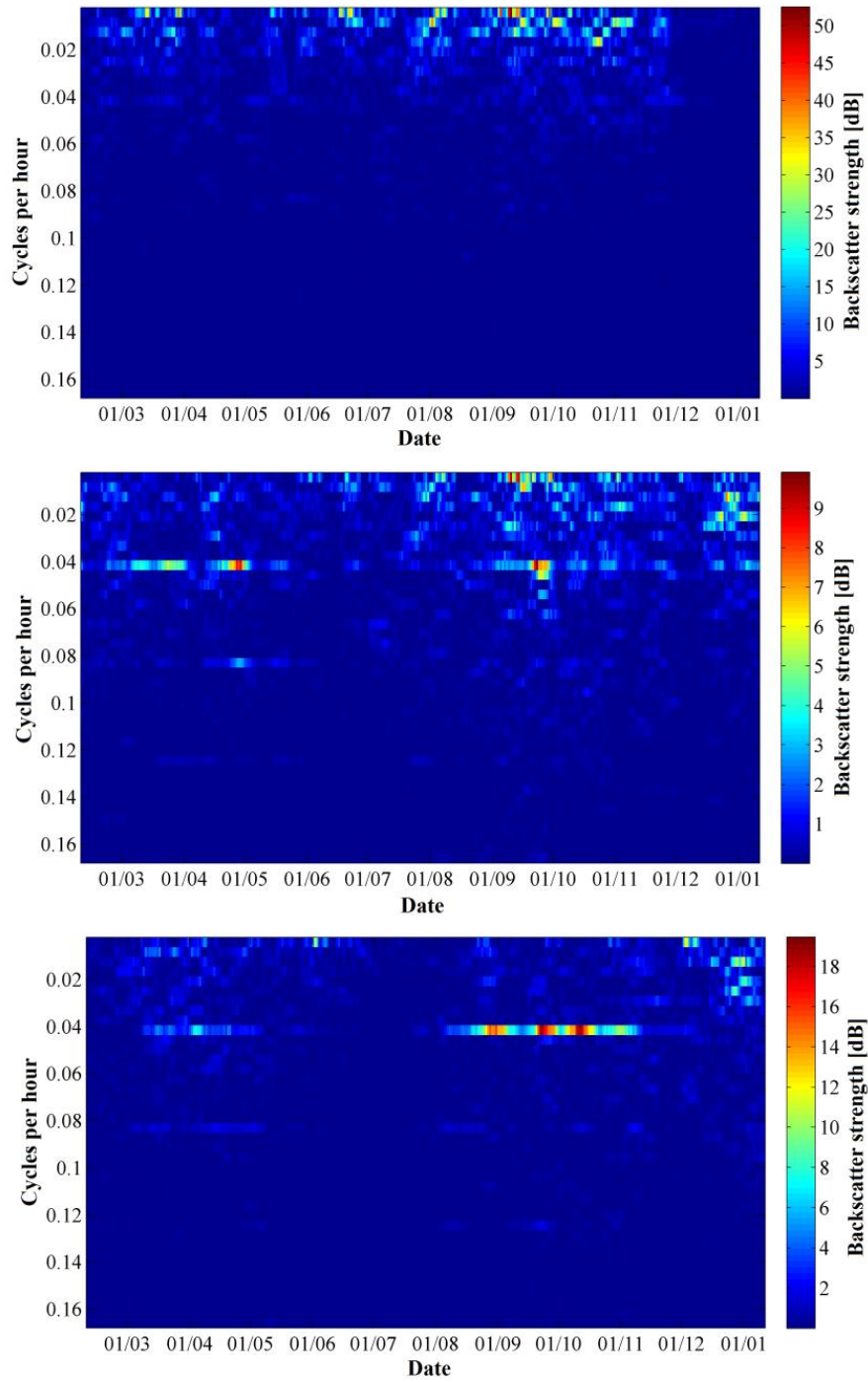


Figure 7. Spectrograms of backscatter strength at 32 m (top), 80 m (middle) and 160 m (bottom). Note the change in scale for the backscatter strength between the panels.

### 3.2 Migratory patterns

To better characterize annual migration patterns, several subsets of hourly backscatter strength data were analysed, corresponding to the clearest 24 h and 12 h peaks of the spectrogram at 160, 80 and 32 m, representing the deep, intermediate and surface layers, respectively. All subsets were

smoothed using a centred three-hour moving average to reduce high frequency variations and noise. During the first period at the end of the polar night, the backscatter signal at 160 m (Figure 8a) demonstrated a strong link between daily variability and the solar cycle. The nights lasted from 18 to 14 hours and the solar radiation was quite low. The absolute minimum in the backscatter signal at 160 m exactly corresponded with the daily light maximum, and the rest of the minima were similar in value. During the night, the cycles were more different from each other, and the value of the maximum value varied, while the relative minimum, indicating the twilight migrations, sometimes was clear, but sometimes hardly appeared. In the upper layers (16-100 m), a daily cycle was clear at the end of the study period, when the time evolution of the backscatter signal was similar at all depths. This suggested an upward migration that affected the entire portion of the water column monitored by the ADCP.

In the second week of September, the backscatter minima tended to coincide with the solar radiation maximum. Three weeks later (Figure 8b), the nights became shorter, lasting 5-10 hours, while the solar radiation increased significantly. Again, there was a very good correspondence between the minima of the backscatter signal at a depth of 160 m and the maxima of the no-sky solar radiation. However, in this subset of the data, the diurnal relative maxima were evident and the nocturnal relative minima were less pronounced overall compared to the previous period. In fact, at the intermediate depth (50-100 m), the backscatter strength did not show an obvious diurnal cycle, indicating that zooplankton tended to remain near the surface.

The third subset of data (Figure 8c) lasted from November 11 to December 1, during the austral summer, and corresponded with the period of maximum intensity in the 24 h harmonic in the upper level, as indicated by the time frequency analysis. During this period, the solar irradiance reached its maxima and light was present at night. Although the daily cycle in the upper layer was more evident during this period and its amplitude was comparable to that of the deep level in spring, the signal was not very clear. On the contrary, during this period, the daily cycle signal in the deeper level showed reduced amplitude, consistent with the results of the time frequency analysis. During autumn (Figure 8d), a clear semidiurnal cycle was observed in the backscatter of the intermediate and deep layers. This might have been due to limited food concentrations, as suggested by Godlewska (1996).

In winter (Figure 8e), no migratory pattern was shown, but in the intermediate and surface levels, the signal showed a variability that might be ascribed to the presence of larvae dwelling near the ice edge (Daly, 1990).



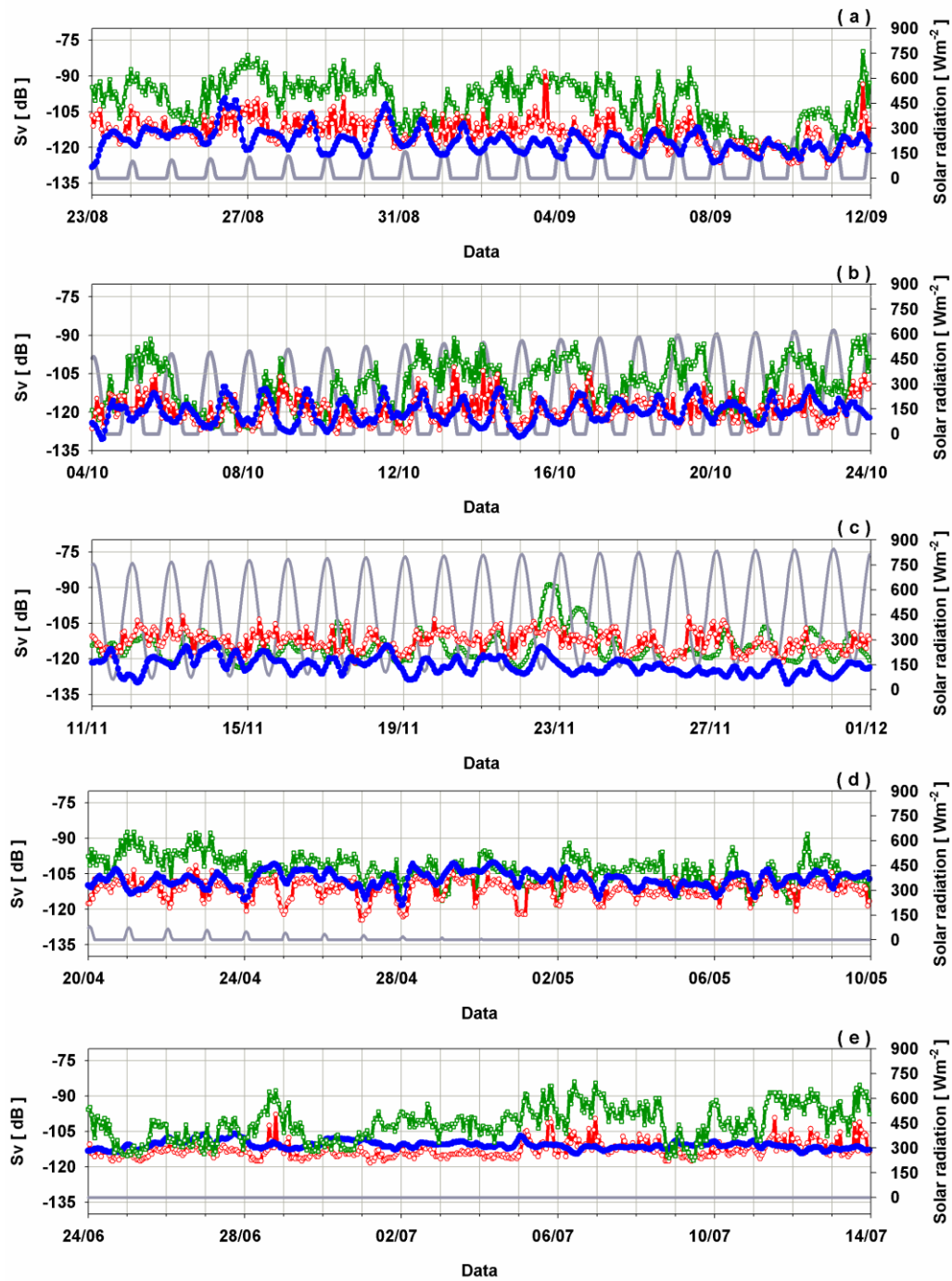


Figure 8. Time series of 20 days during a) August-September, b) October, c) November-December, d) April-May and f) June-July showing the subsets of backscatter strength at 32 m (green line, open squares), 80 m (red line, empty circle) and 160 m (blue line) superimposed on the temporal evolution of no-sky solar radiation (grey solid line).

### 3.3 Diel variability

Analysis of the zooplankton migratory phases showed a strong relationship with the variation in the

duration of daylight. However, the differences in light intensity might also be regarded as a cause of the 24 h upward and downward movements. To investigate the diel variability, the same sub-sets of data used in the previous section were also used here, with the exception of the midnight sun period. For each subset, the hourly mean values of Sv were computed.

The diel variability was detectable when comparing the average Sv to the time of sunset and sunrise. Zooplankton moved towards the surface at sunset and deeper in the water column near sunrise over all periods in which day-night alternated at the mooring site. From the end of August to the middle of September (Figure 9a), sunset and sunrise occurred between 16:11 and 18:17 LT (04:11 to 06:17 UTC) and between 07:37 and 09:54 LT (19:37 and 21:54 UTC), respectively. The diel cycle was clearly defined in the deep layer where the most relevant upward movement corresponded with sunset and the downward movement with sunrise. Sv at 80 m and 32 m showed the same dynamic with an ascent at approximately 18:00 LT (06:00 UTC), roughly two hours after sunset; a downward movement at approximately 03:00 LT (15:00 UTC), followed by a small cycle of 4 hours; and a decrease around sunrise. The duration of the circadian cycle was similar to the sunlight cycle with night lasting for approximately 13 hours.

In the following month (Figure 9b), the length of the night decreased and sunset occurred from 21:13 to 23:36 LT (08:13 to 10:36 UTC) and sunrise from 04:56 to 06:27 LT (14:56 to 17:27 UTC). The curve corresponding to diel variability at 160 m exhibited the same Gaussian shape of the previous period, but it was narrower, and the sharpest movement upward and downward occurred near sunset and sunrise, respectively. Sv at 80 and 32 m were lower than in September, but with a more marked diel cycle. The backscatter strength at the intermediate level was higher than at the deep level only at night.

One month after the March equinox (Figure 9c), it was getting darker, but the zooplankton migration followed the diel cycle, moving upward close to sunset and downward close to sunrise. The time series of all three selected depths exhibited the same trend, with a sharp ascent after sunset to 20:00 LT (08:00 UTC), followed by constant values until one hour before sunrise, at which point a drop occurred. Backscatter strength at 80 m in all periods was lower than the deep level and showed the widest diel cycle. During austral winter, when no sunlight was present (Figure 9d), there was no migration. The backscatter strength at each level exhibited modest variations, with only a few episodes of higher backscatter in the upper level.

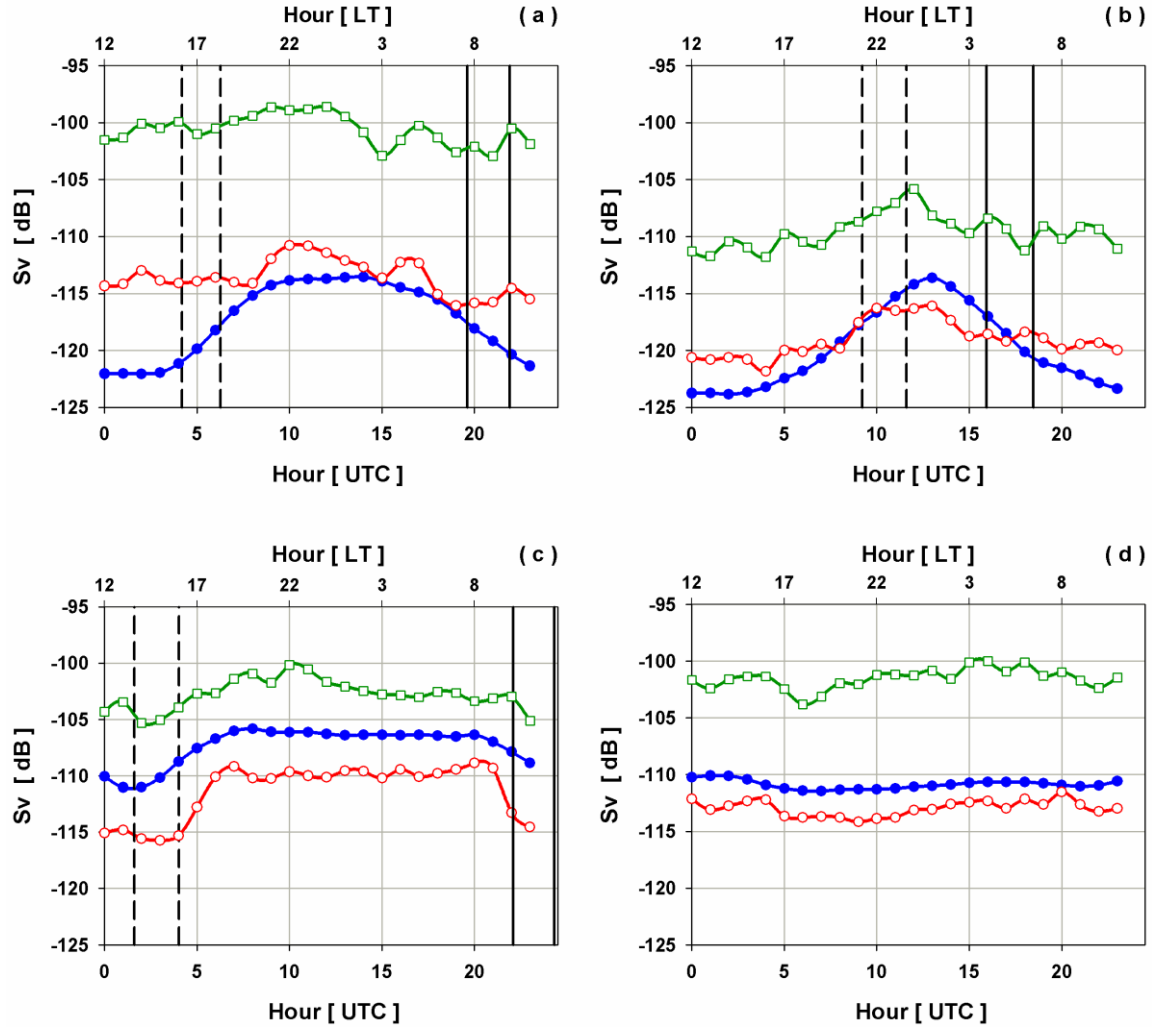


Figure 9. Averaged diel cycles at 160 m (blue filled circles), 80 m (red empty circles) and 32 m (green empty squares) during the following periods: a) 23/8-12/9; b) 4/10-24/10; c) 20/4-10/5; d) 24/6-14/7. Vertical lines indicate sunset (dashed line) and sunrise (solid line) at the beginning and end of each period. Hours are expressed in UTC time and local time (LT=UTC+12 for the New Zealand Standard Time and LT=UTC+13 for the New Zealand Daylight Time) on the lower and upper horizontal axis, respectively.

#### 4. Conclusions

The acoustic backscatter data collected with an ADCP deployed in Terra Nova Bay in 2000 sampled the water column to a depth of 176 m. The ADCP data were originally collected for an entirely different purpose and were re-analysed to investigate zooplankton migrations. Consequently, the one-hour sampling time used here is lower than generally required for this type of application, but it was suitable for performing an accurate spectral analysis. The ADCP worked

at 150 kHz, appropriate for the study of macro-zooplankton and krill, which are an important component of Antarctic zooplankton. Thus, a time frequency analysis allowed for the extraction of useful information from the ADCP data regarding zooplankton dynamics in this area for an entire year.

Assuming that the periodicity of the backscatter signal at 24 h and 12 h periods was related to the diel vertical migration of zooplankton, some information on the seasonal cycle of zooplankton and fish was acquired by analysing the temporal evolution of the amplitude time series as obtained by the FFT analysis. The signal ascribed to the daily migration generally dominated the time series and reached high values. Significant differences were found between the upper 100 m of the water column and the deeper layers (100 - 168 m), both in terms of total backscatter and migration patterns. In the deep layers, the daily signal dominated, but the presence of a sub-daily migration pattern was often detected. Furthermore, the 24 h and the 12 h signals had large amplitudes, even when the measured backscatter data were low, for example, during September and October. This did not occur during December and January, when the backscatter reached maximum values.

The analysis did not reveal any systematic relationship between the backscatter patterns and the physical oceanography of the area. The observed temperature and salinity variability was very small and mainly due to winter dense water formation and summer ice melt. Moreover, the vertical dynamics and the low temporal and spatial resolution of the measurements masked any possible correlation between backscatter signals and vertical velocities. There was a good correlation between the solar annual cycle and migration pattern that was common to all depths, although there was no evidence of a relationship between the time series of the 24 h and 12 h period amplitudes and moon phases. There was a clear link between the ascending-descending zooplankton movement and timing of sunset and sunrise.

During all periods that had a sunrise and sunset, the backscatter strength in the deep layer showed a clear 24 h pattern. There was an increase from sunset until three to four hours later, then a flattening that depended on the duration of night, followed by a sharp decrease near sunrise. The same trend was identifiable in the intermediate level (50-100 m), but was less marked and more variable. The daily migration initiated in late August, just after the end of the polar night, reached a maximum at the beginning of September and then declined. From that time until mid-November, there were three other periods of intense migration, each lasting for approximately ten days. Because the ADCP measurements were not calibrated with in-situ net tows, it was not possible to determine which zooplankton or fish taxa were present. However, it was possible to infer the presence of some species by analysing the relationship between the patterns and season and the hour of sunset-sunrise and daylight length, taking into account knowledge regarding the behaviour of these organisms.

For example, the seasonal distribution of zooplankton is coupled to the reproductive cycle of

*Pleuragramma antarcticum*. During summer, after the phytoplankton bloom, this taxa has a high abundance of its first stage in the surface layer (Granata et al., 2002), while its post-larval and juvenile stages are present down to a depth of 200 m with a progressive decline in abundance (Guglielmo et al., 1998).

From mid-February to the beginning of April 2000, the time series of the 24 h period amplitudes showed an intense migratory phase that could be due to the presence of the ice krill *Euphausia crystallorophias* (Guglielmo et al., 2009). This hypothesis is supported by the analysis carried out by Sala et al. (2002). In that study, during a survey carried out in the Ross Sea between January and February 2000, they found a high concentration of *E. crystallorophias* in the shelf waters and coastal stations close to the mooring site. They suggested that the overall length frequency distribution of *E. crystallorophias* was characterized by a first mode of juvenile individuals and a second mode consisting of sub-adults and adults that perform diel vertical migration. *E. crystallorophias* is a swarming species, which could explain the elevated backscatter strength during the first months of the deployment, when the whole water column was characterized by a diel (24 h and 12 h) vertical migration. During austral winter, the greatest backscatter intensities were collected mainly near the surface, where *E. crystallorophias* completes its larval development (Kirkwood, 1996; Pakhomov and Perissinotto, 1997). In fact, the sea-ice edge could be considered to be a natural nursery habitat that provides refuge from predators (Brierley and Thomas, 2002).

Although many species of Antarctic zooplankton remain active in winter, they limit their vertical migration to maintain a state of metabolic depression (Nicol et al., 2004) or descend to the seabed to feed. The reason for this is the richness of organic matter in the seabed (Smith and Demanster, 2008). This behaviour could be reflected in the simultaneous acquisitions of high backscatter values and the lack of a clear migratory signal.

The low backscatter values observed during the first half of April and spring may be associated with the scatter provided by the presence of copepods, such as *Calanoides acutus*. The life cycle of these copepods consists of a descent to deep levels that corresponds with the increase in sea-ice concentration, a diapause period during winter below 500 m, and an intense migratory phase in springtime when ice melt occurs (Schnack-Schiel et al., 2008). The rapid interchange between low and high backscatter values in early December could be due to a variation in the zooplankton populations following phytoplankton blooms, which usually occur twice in Terra Nova Bay, first between December and January and then in February (Innamorati et al., 2000). In-situ measurements of mesozooplankton biomass collected in December and January by Hernández-León et al. (1999, 2000) revealed a low abundance of copepods and high krill concentrations, confirming the inverse relation between krill and non-krill species identified by several authors (Hosie, 1994; Voronina et al., 1994).

In December and January, the change in Sv values corresponded to an opposite trend in the migratory signal. Similar results were found in the Lazarev Sea by Cisewski et al. (2010). They attributed the strong reduction of migration to a decrease in the zooplankton population or to the limited difference in the daily solar radiation cycle. An additional hypothesis to explain the absence of the diel cycle was proposed by Cottier et al. (2006), which attributed the lack of migration to a chaotic up and down motion of the zooplankton to both feed and escape from predators.

Acoustic backscatter data were limited to the upper 176 m of the water column. Although the major density of euphausiids and copepods remains in the surface layers during the spring and summer months (Pane et al., 2004), it was not possible to investigate the change in density with depth or the possible descent of zooplankton to the sea floor due to the mooring configuration. Consequently, the hypothesis of copepod diapause is based on knowledge of their general behaviour.

The analysis of the time series of backscatter data performed in the time frequency domain allowed zooplankton migrations to be identified in an automated and objective way. This analytical method is a simple but efficient technique to extract useful biological information from ADCP observations. This suggests that other available long-term acoustics data, even if obtained from non-dedicated, low-resolution instruments, could provide additional time series data of biological relevance and significantly improve ecosystem dynamics and productivity studies. They are of particular interest in polar regions where direct observations are scarce and difficult to obtain. Thus, it would be valuable to include ADCP data in existing environmental observing systems.

## **Acknowledgments**

Methods for data analysis were tested in the framework of the project “Development and test of underwater acoustic methods for the remote monitoring of air-sea-ice interaction processes in polynya”, Contract PNRA 2010/A4.01. ADCP and CTD data were collected in the framework of the PNRA- CLIMA (Climatic Long-term Interactions for the Mass balance in Antarctic) Project. This work was also partially funded by the Flagship Project RITMARE, The Italian Research for the Sea, coordinated by the Italian National Research Council and funded by the Italian Ministry of Education, University and Research within the National Research Program 2011–2013. The authors are grateful to Dr. Gabriele Buondonno (University of Rome) for useful discussions.

## **References**

Accornero, A., Manno, C., Esposito, F., Gambi, M.C., 2003. The vertical flux of particulate matter in the polynya of Terra Nova Bay. Part II Biological component. *Antarctic Science* 15, 175-188.

doi:10.1017/S0954102003001214.

Ainslie, M.A., Mc Colm, J.G., 1998. A simplified formula for viscous and chemical absorption in seawater. *Journal of the Acoustical Society of America* 103 (3),1671–1672.doi: 10.1121/1.421258.

Antarctic Treaty Secretariat, 2003. Antarctic Specially Protected Area no 161,Terra Nova Bay, Ross Sea, Final Report of XXVI ATCM, 225-238.

Assmann, K.M., Timmermann, R., 2005. Variability of dense water formation in the Ross Sea. *Ocean Dynamics*55, 68–87. doi: 10.1007/s10236-004-0106-7.

Azzali, M., Kalinowski, J., 2000. Spatial and temporal distribution of krill (*Euphausia superba*) biomass in the Ross Sea (1989-1990 and 1994), in: Faranda, F. M., Guglielmo, L. and Ianora, A. (Eds.), *Ross Sea Ecology. Italianantartide Expeditions (1987–1995)*. Springer Verlag, Berlin. 433-345. doi: 10.1007/978-3-642-59607-0\_31.

Blanc, S., Baquès, M., Etcheverry de Milou, M.I., 2008. Examining the plankton acoustic response with a vessel mounted ADCP across oceanic fronts located in the Drake Passage, *Geoacta* 33, 110-121.

Bozzano, R., Fanelli, E., Pensieri, S., Picco, P., Schiano, M.E., 2014. Temporal variations of zooplankton biomass in the Ligurian Sea inferred from long time series of ADCP data. *Ocean Science* 10, 93-105.doi:10.5194/os-10-93-2014.

Brierley, A.S., Thomas, D.N., 2002. Ecology of Southern Ocean pack ice. *Adv. Mar. Biol.* 43,171–276. doi: 10.1016/S0065-2881(02)43005-2.

Brierley, A.S., Saunders, R. A., Bone, D.G., Murphy, E. J., Enderlein, P., Conti, S. G., Demer, D.A., 2006. Use of moored acoustic instruments to measure short-term variability in abundance of Antarctic krill. *Limnology and Oceanography: Methods* 4, 18-29. doi:10.4319/lom.2006.4.18.

Briseño-Avena, C., Roberts, P. L.D., Franks, P.J.S., Jaffe, J. S., 2015. ZOOPS-O2: A broadband echosounder with coordinated stereo optical imaging for observing plankton in situ. *Methods in Oceanography* 12, 36–54. doi: 10.1016/j.mio.2015.07.001.

Cappelletti, A., Picco, P., Peluso, T., 2010. Upper ocean layer dynamics and response to atmospheric forcing in the Terra Nova Bay polynya, Antarctica. *Antarctic Science* 22(3), 319–329. doi:10.1017/S095410201000009X.

Carli, A., Pane, L., Stocchino, C., 2000. Planktonic Copepods in Terra Nova Bay (Ross Sea): distribution and relationship with environmental factors, in: Faranda, F.M., Guglielmo, L. and Ianora, A. (Eds.), *Ross Sea Ecology. Italian Antarctic Expeditions (1987–1995)*. Springer Verlag, Berlin, 309–321. doi:10.1007/978-3-642-59607-0\_24.

Cavalieri, D.C., Parkinson, C., Gloersen, P., Zwally, H.J., 1996, updated 2008. Sea-ice concentration from Nimbus-7 SMMR and DMSP SSM/I passive microwave data. Boulder, CO: National Snow and Ice Data Center. Digital Media. doi:10.5067/8GQ8LZQVL0VL.

Cisewski, B., Strass, V.H., Rhein, M., Krägefsky, S., 2010. Seasonal variation of diel vertical migration of zooplankton from ADCP backscatter time series data in the Lazarev Sea, Antarctica. *Deep-Sea Research Part I-Oceanographic Research Papers* 57(1), 78-94. doi: 10.1016/j.dsr.2009.10.005.

Cottier, F.R., Tarling, G.A., Wold, A., Stig, F.P. 2006. Unsynchronised and synchronised vertical migration of zooplankton in a high Arctic fjord. *Limnology and Oceanography* 51, 2576-2599. doi:10.4319/lo.2006.51.6.2586.

Daly, K.L., 1990. Overwintering development, growth, and feeding of larval *Euphausia superba* in the Antarctic marginal ice zone. *Limnology and Oceanography* 35, 1564-1576. doi:10.4319/lo.1990.35.7.1564.

Fielding, S., Griffiths, G., Roe, H.S.J., 2004. The biological validation of ADCP acoustic backscatter through direct comparison with net samples and model predictions based on acoustic-scattering models. *Journal of Marine Sciences* 61 (2), 184-200. doi:10.1016/j.icesjms.2003.10.011.

Flagg, C.M., Smith, S.L., 1989. On the use of the Acoustic Doppler Current Profiler to measure zooplankton abundance. *Deep-Sea Research I* 36, 455-474. doi:10.1007/BF00346352.

Godlewska, M. 1996. Vertical migrations of krill (*Euphausia superba* Dana). *Polish Archives of Hydrobiology* 14, 9-63.



Gostiaux, L., van Haren, H., 2010. Extracting meaningful information from uncalibrated backscattered echo intensity data. *Journal of Atmospheric and Oceanic Technology* 27, 943–949. doi:10.1175/2009JTECHO704.1.

Granata, A., Cubeta, A., Guglielmo, L., Sidoti, O., Greco, S., Vacchi, M., La Mesa, M., 2002. Ichthyoplankton abundance and distribution in the Ross Sea during 1987-1996. *Polar Biology*, 25(3), 187-202. doi: 10.1007/s00300-001-0326-y.

Guglielmo, L., Granata, A., Greco, S., 1998. Distribution and abundance of postlarval and juvenile *Pleuragramma antarcticum* (Pisces, Nototheniidae) off Terra Nova Bay (Ross Sea, Antarctica). *Polar Biology*, 19(1), 37-51. doi:10.1007/s0030000050214.

Guglielmo, L., Donato, P., Zagami, G., Granata, A., 2009. Spatio-temporal distribution and abundance of *Euphausia crystallorophias* in Terra Nova Bay (Ross Sea, Antarctica) during austral summer. *Polar Biology*, 32(3), 347-367. doi:10.1007/s00300-008-0546-5.

Hernández-León, S., Torres, S., Gómez, M., Montero, I., Almeida, C., 1999. Biomass and metabolism of zooplankton in the Bransfield Strait (Antarctic Peninsula) during austral spring. *Polar biology*, 21(4): 214-219. doi: 10.1007/s0030000050355.

Hernández-León, S., Almeida, C., Portillo-Hahnefeld, A., Gómez, M., Montero, I., 2000. Biomass and potential feeding, respiration and growth of zooplankton in the Bransfield Strait (Antarctic Peninsula) during austral summer. *Polar biology*, 23(10): 679-690. doi:10.1007/s0030000000139.

Hopkins, T.L., 1987. Midwater food web in McMurdo Sound, Ross Sea, Antarctica. *Marine Biology*, 96(1), 93-106. doi:10.1007/BF00394842.

Hosie, G.W., Cochran, T.G., 1994. Mesoscale distribution patterns of macrozoo-plankton communities in Prydz Bay, Antarctica January to February 1991. *Mar. Ecol. Prog. Ser.* 106, 21–39. doi: 10.3354/meps106021.

Hyatt, J., Visbeck, M., Beardsley, R.C., Owens, W.B., 2008. Estimating sea-ice coverage, draft, and velocity in Marguerite Bay (Antarctica) using a subsurface moored upward-looking Acoustic Doppler Current Profiler (ADCP). *Deep Sea Research II* 55, 351–364. doi:

10.1016/j.dsr2.2007.11.004.

Innamorati, M., Mori, G., Massi, L., 2000. Phytoplankton biomass related to environmental factors in the Ross Sea, in: Faranda, F. M., Guglielmo, L. and Ianora, A. (Eds.), Ross Sea Ecology. Italian Antarctic Expeditions (1987–1995). Springer Verlag, Berlin, 217–230. doi:10.1007/978-3-642-59607-0\_18.

Jacobs, S.S., Fairbanks, R.G. Horibe, Y., 1985. Origin and evolution of water masses near the Antarctic continental margin: evidence from H<sub>2</sub>18O/ H<sub>2</sub>16O ratios in seawater. in Oceanology of the Antarctic Continental Shelf. Antarctic Research Series, Vol. 43, Am. Geophys. Union, Washington, DC (1985), 59–85.

Jacobs, S.S., 2004. Bottom water production and its links with the thermohaline circulation. Antarctic Science 16(4), 427–437. doi: 10.1017/S095410200400224X.

Jourdin, F., Tessier, C., Le Hir P., Verney, R., Lunven, M., Loyer, S., Lusven, A., Filipot, J.F., Lepasqueur, J., 2014. Dual-frequency ADCPs measuring turbidity. Geo-Marine Letters 34, 381–397. doi: 10.1007/s00367-014-0366-2.

Karnowsky, N., Ainley, D.G., Lee, P., 2007. The impact and importance of production in polynyas to top-trophic predators: three case histories, in: Polynyas, window to the world. Smith, W.O., Barber, D. (Eds.), Elsevier, 391–410. doi:10.1016/S0422-9894(06)74012-0.

Kirkwood, J. M, 1996. The developmental rate of *Euphausia crystallorophias* larvae in Ellis Fjord, Vestfold Hills, Antarctica. Polar Biology 16(7), 527–530. doi=10.1007/BF02329073.

Kooyman, G.L., Croll D., Ston, S., Smith, S., 1990. Emperor penguin colony at Cape Washington, Antarctica Polar Record 26, 103–108.

Kurtz, D. D., Bromwich, D. H., 1985. A Recurring, Atmospherically Forced Polynya in Terra Nova Bay, in Oceanology of the Antarctic Continental Shelf (ed S. S. Jacobs), American Geophysical Union, Washington, D. C., 177–201. doi: 10.1029/AR043p0177.

Lemon, D., Johnston, P., Buermans, J., Loos, E., Borstad, G., Brown, L., 2012. Multiple-frequency moored sonar for continuous observation of zooplankton and fish. Proc. MTS/IEEE International

Conference Oceans 2012. doi:10.1109/OCEANS.2012.6404918.

Nicol, S., Virtue, P., King, R., Davenport, S.R., McGaffin, A.F., Nichols, P., 2004. Condition of *Euphausia crystallorophias* off East Antarctica in winter in comparison to other seasons. Deep-Sea Research Part II: Topical Studies in Oceanography, 51(17-19), 2215-2224. doi:10.1016/j.dsr2.2004.07.002.

Pakhomov, E.A., Perissinotto, R., 1997. Spawning success and grazing impact of *Euphausia crystallorophias* in the Antarctic shelf region, in Antarctic Communities: Species, Structure and Survival (ed. B. Battaglia, J. Valencia, D.W.H. Walton), Cambridge University Press, UK, 187-192.

Pane, L., Feletti, M., Francomacaro, M., Mariottini, G.L., 2004. Summer coastal zooplankton biomass and copepod community structure near the Italian Terra Nova Base (Terra Nova Bay, Ross Sea, Antarctica). Journal of Plankton Research 26(12), 1479-1488.

Pinkerton, M.H., Bradford-Grieve, J.M., Hanchet, S.M., 2010. A balanced model of the food web of the Ross Sea, Antarctica. CCAMLR Science 17, 1–31. doi: 10.1093/plankt/fbh135.

PNRA, 2001. Rapporto sulla Campagna Antartica Estate Australe 2000–2001, XVI Spedizione. Roma: ProgettoAntartide, ANT 01/01, 259 pp.

RD Instruments, 1998. Calculating absolute backscatter in narrowband ADCPs. RDI Field Service Technical Paper FST-003, San Diego, CA, 24 pp.

Russo, C.R., Boss, E.S., 2012. An Evaluation of Acoustic Doppler Velocimeters as Sensors to Obtain the Concentration of Suspended Mass in Water. Journal of Atmospheric and Oceanic Technology 29, 755-761. doi: 10.1175/JTECH-D-11-00074.1.

Sala, A., Azzali, M., Russo, A., 2002. Krill of the Ross Sea: distribution, abundance and demography of *Euphausia superba* and *Euphausia crystallorophias* during the Italian Antarctic Expedition (January-February 2000). Scientia Marina, 66(2): 123-133. doi:10.3989/scimar.2002.66n2123.

Schnack-Schiel, S.B., Michels, J., Mizdalski, E., Schodlok, M.P., Schröder, M., 2008. Composition

and community structure of zooplankton in the sea ice-covered western Weddell Sea in spring 2004-with emphasis on calanoid copepods. *Deep-Sea Research Part II: Topical Studies in Oceanography*, 55(8-9): 1040-1055. doi: 10.1016/j.dsr2.2007.12.013.

Smith, C.R., Demaster, D. J. 2008. Preface and brief synthesis for the FOODBANCS volume; *Deep-Sea Research Part 2. Topical studies in oceanography* 55, 2399-2403.doi:10.1016/j.dsr2.2008.08.001.

Soares, C.G., Cherneva, Z., 2005. Spectrogram analysis of the time–frequency characteristics of ocean wind waves. *Ocean Engineering* 32(14-15), 1643-1663. doi: 10.1016/j.oceaneng.2005.02.008.

Tagliabue, A., Arrigo, K.J., 2003. Anomalously low zooplankton abundance in the Ross Sea: An alternative explanation. *Limnology and Oceanography* 48(2),686–699. doi:10.4319/lo.2003.48.2.0686.

Tremblay, J.E., Smith, W.O., 2007. Primary production and nutrient dynamics in polynyas. In: *Polynyas, window to the world*. Smith, W.O., Barber, D. (Eds.), Elsevier 239-269.doi:10.1016/S0422-9894(06)74008-9.

Vacchi, M., DeVries, A. L., Evans, C. W., Bottaro, M., Ghigliotti, L., Cutroneo, L., Pisano, E., 2012. Nursery area for the Antarctic silverfish *Pleuragramma antarcticum* at Terra Nova Bay (Ross Sea): first estimate of distribution and abundance of eggs and larvae under the seasonal sea-ice.*Polar Biology* 35, 1573–1585. doi:10.1007/s00300-012-1199-y.

van Haren, H., 2001. Estimates of sea level, waves and winds from a bottom-mounted ADCP in a shelf sea. *Journal of Sea Research*, 45, 1-14. doi: 10.1016/S1385-1101(00)00060-5.

van Haren, H., 2007. Monthly periodicity in acoustic reflection and vertical motion in the deep ocean. *Geophysical Research Letters* 34, L12603. doi:10.1029/2007GL029947.

van Woert, M.L., 1999. Wintertime dynamics of the Terra Nova Bay polynya. *Journal of Geophysical Research*104, 7753–7769. doi:10.1029/1999JC900003.

Visbeck, M., Fisher, J., 1995. Sea surface conditions remotely sensed by upward-looking ADCPs.

Journal of Atmospheric and Oceanic Technology 12, 141–149. doi:10.1175/1520-0426(1995)012<0141:SSCRSB>2.0.CO;2.

Voronina, N.M., Kosobokova, K.N., Pakhomov, E.A., 1994. Composition and biomass of summer metazoan plankton in the 0–200 m layer of the Atlantic sector of the Antarctic. *Polar Biology*, 14 (2), 91-95. doi: 10.1007/BF00234970.

Depth limits of each bin [m]	152-168	136-152	120-136	104-120	88-104	72-88	56-72	40-56	24-40	8-24
<div>Bin</div> <div>Bin</div>	1	2	3	4	5	6	7	8	9	10
1	1 0	0.94 0	0.87 0	0.73 0	0.6 0	0.49 0	0.26 0	0.52 0.0007	-0.04 0.0043	-0.12 0.9972
2		1 0	0.97 0	0.86 0	0.72 0	0.57 0	0.28 0	0.03 0.0057	-0.09 0.3779	-0.13 0.5776
3			1 0	0.95 0	0.85 0	0.70 0	0.38 0	0.08 0.0009	-0.08 0.4613	-0.10 0.6426
4				1 0	0.96 0	0.82 0	0.51 0	0.14 0	-0.05 0.2943	-0.07 0.8878
5					1 0	0.93 0	0.64 0	0.27 0	0.03 0	0.02 0
6						1 0	0.86 0	0.53 0	0.28 0	0.26 0
7							1 0	0.86 0	0.67 0	0.61 0
8								1 0	0.93 0	0.86 0
9									1 0	0.92 0
10										1 0

Table 1. Correlation matrix of backscatter strength. Correlation coefficients, R and P values computed with an alpha set to 0.05, are shown in the first and second rows of each cell, respectively. Values lower than 10<sup>-4</sup> are rounded to 0.